Rock Mechanics and Rock Engineering (2021) 54:973–980
https://doi.org/10.1007/s00603-020-02277-y

TECHNICAL NOTE

Identifying Accurate Crack Initiation and Propagation Thresholds in Siliceous Siltstone and Limestone

Xiao-Ping Zhang[1,2] · Gen-Gen Lv[1,2] · Quan-Sheng Liu[1,2] · Shun-Chuan Wu[3,4] · Qi Zhang[1,2] · Pei-Qi Ji[1,2] · Xu-Hai Tang[1,2]

Received: 19 March 2019 / Accepted: 12 October 2020 / Published online: 28 October 2020

Keywords Crack initiation · Stress–strain curve · Stress thresholds · Acoustic emission monitoring

List of Symbols

σ_{cc}	Crack closure stress
σ_{ci}	Crack initiation stress
σ_{cd}	Crack damage stress
σ_f	Peak strength
ε_v	Volumetric strain
ε_{ve}	Elastic volumetric strain
ε_{vc}	Crack volumetric strain
ΔV	Change of specimen volume
$\Delta V_{elastic}$	Change of elastic volume
ε_{axial}	Axial strain
$\varepsilon_{lateral}$	Lateral strain
E	Elastic modulus
ν	Poisson's ratio
P wave	Pressure wave
σ_1	Maximum loading stress
σ_3	Minimum loading stress

Abbreviations

AE	Acoustic emission
CVS	Crack volumetric strain method
LSR	Lateral strain response method
MPR	Moving point regression method

✉ Xiao-Ping Zhang
jxhkzhang@163.com

✉ Quan-Sheng Liu
liuqs@whu.edu.cn

1 Key Laboratory of Safety for Geotechnical and Structural Engineering of Hubei Province, School of Civil Engineering, Wuhan University, Wuhan 430072, China

2 State Key Laboratory of Water Resources and Hydropower Engineering Science, Wuhan University, Wuhan 430072, Hubei, China

3 Faculty of Land Resources Engineering, Kunming University of Science and Technology, Kunming, Yunnan 650093, China

4 School of Civil and Resource Engineering, University of Science and Technology Beijing, Beijing 100083, China

1 Introduction

Deep buried tunnels often suffer brittle instability and failure during the excavation process under high geological stress conditions (Liu et al. 2018). During this process, the surrounding rocks partially begin to break with crack initiation and growth. The deformation and failure of brittle rocks is a gradual process involving the initiation, growth and aggregation of cracks (Martin and Chandler 1994). The deformation and failure process of brittle rocks has been widely concerned by many researchers (Dai et al. 2015; Yang 2016; Yang and Hu 2019; Yang et al. 2018; Zhang and Wong 2013; Zhang et al. 2017; Zhou et al.2015). Researchers studied the failure of brittle rocks and divided the stress–strain curves of brittle rocks into five stages: stage I-crack closure; stage II-linear elastic deformation; stage III-crack initiation and stable crack growth; stage IV-unstable crack growth; and stage V-failure and post-peak behavior (Wawersik and Brace 1971; Eberhardt et al. 1999; Hoek and Bieniawski 1965; Scholz 1968; Zhou et al. 2014; Cheng et al. 2016; Zhang et al. 2011; Hallbauer et al. 1973; Tapponnier and Brace 1976). These five stages of the stress–strain curve are divided by four stress thresholds: crack closure stress (σ_{cc}), crack initiation stress (σ_{ci}), crack damage stress (σ_{cd}) and peak strength (σ_f). The crack closure stress (σ_{cc}) indicates the closing of the preexisting microcracks within the rock; the crack initiation stress (σ_{ci}) indicates the beginning of newborn microcracks within the rock; the crack damage stress (σ_{cd}) characterizes the coalescing of the nascent microcracks, which means the specimen loads into the unstable crack growth stage.

To accurately obtain the stress thresholds, many methods have been proposed by researchers. Brace et al. (1966)

studied the crack initiation and growth of granite, marble and aplite. These authors stated that the crack initiation stress is the deflected point from linearity and the onset of dilatancy in the stress–volumetric strain curve. Lajtai (1974) noted that lateral strain was more sensitive than axial strain in response to fracture development. Lajtai (1974) proposed to define the point where the lateral strain curve deviates from the linear section as the initiation stress. Martin and Chandler (1994) explored the failure of Lac du Bonnet granite and obtained the stress thresholds by calculating the total volumetric strain and the crack volumetric strain. Eberhardt et al. (1998) and Zhao et al. (2012) explored the relationship between crack initiation and growth and acoustic emission in brittle rock uniaxial compression. These studies indicated that the properties of acoustic emission response were significantly different before and after the crack initiation stress and the crack damage stress. The moving point regression method was also developed to establish the crack closure stress and the crack initiation stress. Nicksiar and Martin (2012) introduced the lateral strain response method to identify the crack initiation stress in igneous rocks, sedimentary rocks and metamorphic rocks. These studies showed that the crack initiation stress of those rocks occurs at 0.42–0.47 of the peak stress under uniaxial compression.

Due to the unloading after excavation/drilling and stress redistribution, the surface of the tunnel is the stress concentration region. As shown in Fig. 1, the axial stress σ_r reduced to 0 after tunnel excavation while the tangential stress σ_θ increased to a certain value. So, the stress concentration region on the tunnel surface is approximately under uniaxial compression. Hence, the reliable stress thresholds under uniaxial compressive test are critically important for evaluating the failure state and designing the support of surrounding rock. Nevertheless, it is difficult to precisely determine the stress thresholds. At present, there is no unified solution method worldwide. In the present study, siliceous siltstone and limestone are used as examples to carry out stress–strain measurement and acoustic emission evaluation during uniaxial compression tests and to compare and analyze several methods for obtaining reliable stress thresholds.

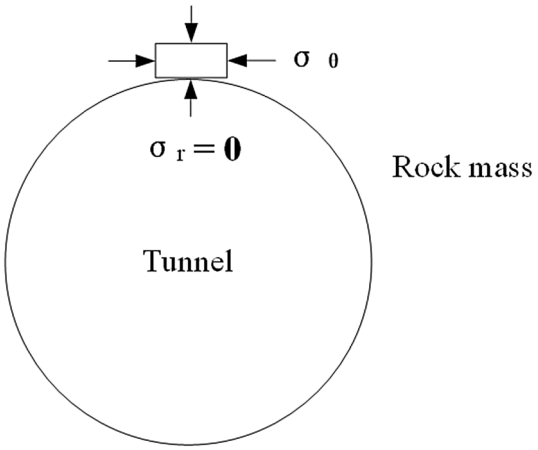

Fig. 1 Stress condition on the tunnel surface after excavation

2 Experimental Procedure

The uniaxial compressive tests were carried out on specimens of siliceous siltstone and limestone in the laboratory of Wuhan University, China. The siliceous siltstone and limestone were taken from the tunnels of the two water transfer projects in Xinjiang Uygur Autonomous Region and Changchun city, China, respectively. The specimens were carefully prepared by cutting and polishing as cylindrical specimens with ϕ 50 mm × H 100 mm. The average density and P wave velocity of siliceous siltstone and limestone are shown in Table 1. The tests were conducted by increasing the strain at 0.001 mm/s on the test specimen using the RMT-301 rock mechanics testing system housed at the Wuhan University. Four displacement sensors were utilized to monitor the deformation and failure behavior of the specimens. The acoustic emission signals generated by the initiation and propagation of internal microcracks in specimen loading were monitored by the test PCI-2 multichannel AE detection system and the NANO-30 type AE sensors (Zhang and Zhang 2017). The frequency of the AE sensors was in the range of 100–400 kHz. The threshold was set at 45 dB, and a gain of 40 dB was used in the experiments. Before the experimental test, the ends of the specimens were greased to reduce the effects of end confinement. The experimental setup for strain measurements (displacement sensors) and AE monitoring (AE sensors) is shown in Fig. 2.

Table 1 Physical and mechanical properties of tested specimens

Rock type	Density (g/cm^3)	P wave (m/s)	Uniaxial compressive strength (MPa)	Elastic modulus E(GPa)	Poisson's ratio, ν
Siliceous siltstone	2.89	4340	217.3	75.9	0.10
Limestone	2.50	2900	131.1	26.1	0.21

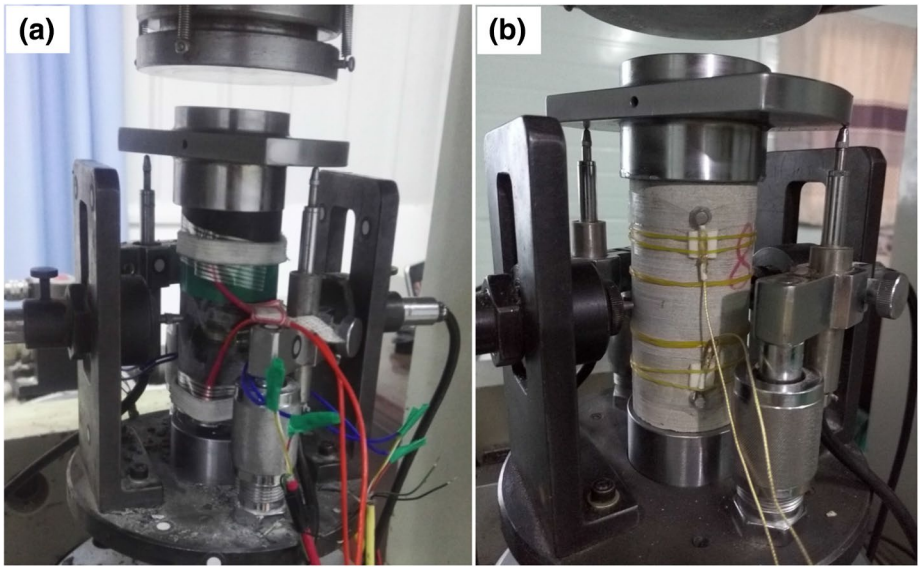

Fig. 2 Experimental setup for uniaxial compressive strength tests with acoustic emission monitoring of **a** siliceous siltstone and **b** limestone

3 Methods of Obtaining the Rock Stress Thresholds

3.1 Crack Volumetric Strain Method (CVS)

Martin and Chandler (1994) performed a series of damage-controlled tests on specimens of Lac du Bonnet granite. These authors suggested that the volumetric strain (ε_v) of rock compression can be divided into two parts: elastic volumetric strain (ε_{ve}) and crack volumetric strain (ε_{vc}). The elastic modulus E and Poisson's ratio μ are calculated by elastic segment (stage II). Elastic volumetric strain is calculated using formula (1):

$$\varepsilon_{ve} = \frac{\Delta V}{\Delta V_{elastic}} = \frac{1-2\mu}{E}\left(\sigma_1 - \sigma_3\right) \tag{1}$$

where ΔV is the change in specimen volume and $\Delta V_{elastic}$ is the change inelastic volume.

Under uniaxial compression, $\sigma_3 = 0$. Then, the volumetric strain is calculated using the axial strain and lateral strain:

$$\varepsilon_v = \Delta V/V \approx \varepsilon_{axial} + 2\varepsilon_{lateral} \tag{2}$$

where ε_{axial} is the axial strain and $\varepsilon_{lateral}$ is the lateral strain.

The crack volumetric strain is calculated using formula (3):

$$\varepsilon_{vc} = \varepsilon_v - \varepsilon_{ve} \tag{3}$$

The crack initiation stress (σ_{ci}) is the starting point of the stress–strain curve from the crack initiation stage to the stable crack growth stage. The loading strength corresponds to the crack initiation stress (σ_{ci}) when the crack volumetric strain curve changes from zero to a negative value. The lateral strain–axial stress curve changes from linear to nonlinear from the crack initiation stress (σ_{ci}) as shown in Fig. 3. The newborn cracks do not increase unless the axial load is increased. The crack initiation stress (σ_{ci}) is difficult to determine using the stress–strain curve, especially for specimens with many preexisting cracks. The crack damage stress (σ_{cd}) is the reversal point in the volumetric strain curve. The volumetric strain reaches its maximum value and turns from compression to dilation, which represents the beginning of the unstable crack growth stage. It shows a significant increase in the strain rate in the axial strain–stress curve. The main reason is that the adjacent tensile cracks are connected with each other and the shear band is gradually formed, which eventually leads to the macroscopic damage. The results of the crack volumetric strain method are shown in Table 2.

The crack closure stress (σ_{cc}) is the axial stress where the crack volumetric strain approaches stability. The axial stress reaches the crack initiation stress (σ_{ci}) when the crack volumetric curve decreases to a negative value. The crack damage stress (σ_{cd}) is the reversal point of the volumetric strain curve. These characteristic stresses (σ_{cc}, σ_{ci}, σ_{cd}, σ_f) of the siliceous siltstone and limestone are marked in Fig. 3. The stress thresholds of these specimens are 22% (σ_{cc}/σ_f), 47% (σ_{ci}/σ_f), 98% (σ_{cd}/σ_f) of peak stress (siliceous siltstone), and 30% (σ_{cc}/σ_f), 50% (σ_{ci}/σ_f), 98% (σ_{cd}/σ_f) of peak stress (limestone), respectively. However, the value of crack closure stress (σ_{cc}) and crack initiation stress (σ_{ci}) will be clearly changed by small fluctuations of Poisson's ratio. Nevertheless, this result shows that the nonlinear change in lateral strain makes the measurement of Poisson's ratio complicated (1998). Different Poisson's ratios corresponding to the crack volume curves are shown in Fig. 4.

It can be seen from the figure that the volumetric strain curve of the cracks solved by different Poisson's ratios is

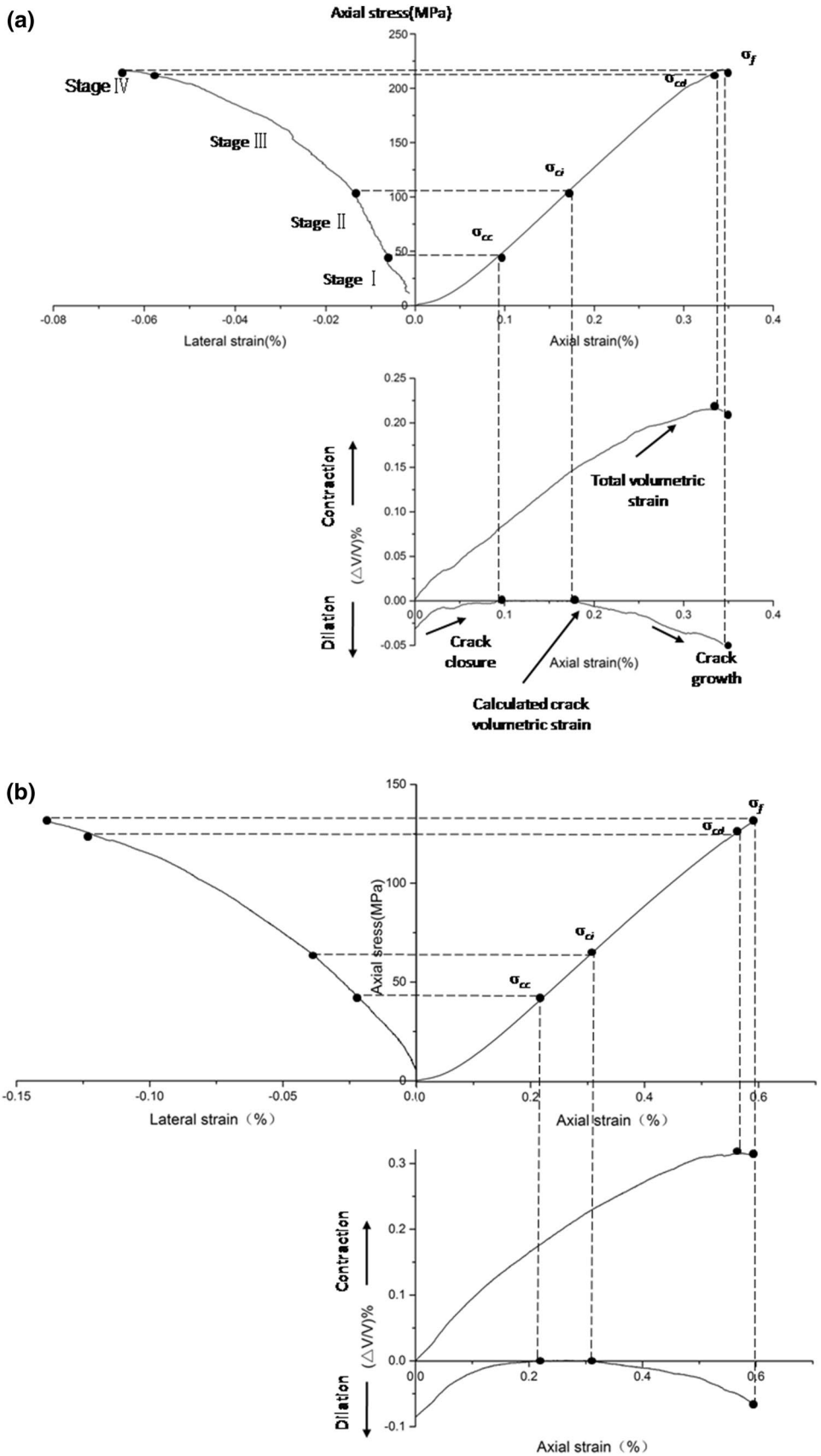

Fig. 3 Curves of axial stress, total volumetric strain and calculated crack volumetric strain versus axial strain obtained from **a** siliceous siltstone and **b** limestone. Stages I, II, III and IV represent crack closure, elastic deformation, crack initiation and stable crack growth, unstable crack growth to failure, respectively

Table 2 Result of the stress thresholds obtained by the crack volumetric strain method

Rock type	Stress threshold(MPa)			Stress ratio	
	σ_{ci}	σ_{cd}	σ_f	σ_{ci}/σ_f	σ_{cd}/σ_f
Siliceous siltstone	102.90	214.47	217.3	0.47	0.98
Limestone	65.26	128.63	131.1	0.50	0.98

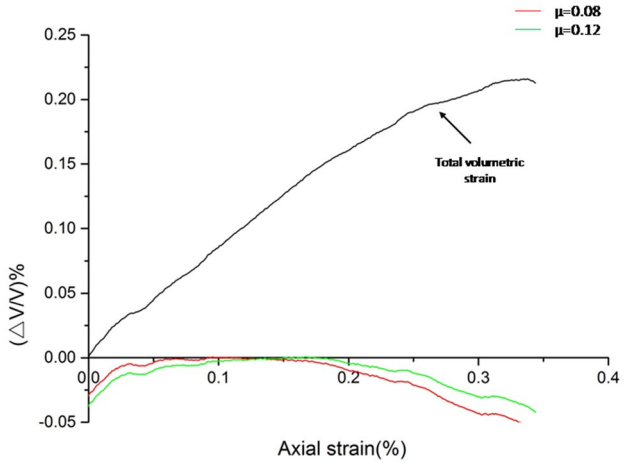

Fig. 4 Crack volumetric strains calculated by different values of Poisson's ratio for siliceous siltstone

Table 3 Result of the stress thresholds obtained by different values of Poisson's ratio

Poisson's ratio, μ	σ_{cc} (MPa)	σ_{ci} (MPa)
0.08	44.75	63.29
0.12	77.54	107.88

approximately similar. The differences are the position of the curves approaching the zero point (σ_{cc}) and the position of the deviation from the zero point (σ_{ci}). In Fig. 4, when different values of Poisson's ratio are taken, the points of σ_{cc} and σ_{ci} are significantly different. In general, the larger the value of Poisson's ratio that is calculated, the larger the crack initiation stress is. Table 3 shows the results of different values of Poisson's ratio for solving σ_{cc} and σ_{ci}. Therefore, when the fracture volumetric strain method is used to solve the crack initiation stress, it is necessary to objectively determine the value of Poisson's ratio that is relatively correct to avoid large errors due to differences in the value of Poisson's ratio.

3.2 Lateral Strain Response Method (LSR)

Nicksiar and Martin (2012) proposed the LSR to obtain the crack initiation stress (σ_{ci}). These authors obtained the value by calculating the difference between the lateral strain and the reference line (Fig. 5). Then, polynomial fitting is performed on the value, and the peak point of the fitting curve corresponds to the crack initiation stress (σ_{ci}). First, by analyzing the axial stress–total volumetric strain curve, the maximum point in the volumetric strain curve is obtained, which corresponds to the crack damage stress (σ_{cd}). In the axial stress–lateral strain curve, the crack damage stress point and zero point are selected as a reference line. At the same axial stress level, the actual lateral strain is subtracted from the reference line to solve the lateral strain difference, and the relationship between the lateral strain difference and the axial stress is plotted. By polynomial fitting of the data points, the maximum value of the fitting curve is the crack initiation stress (σ_{ci}).

The key to determine the crack initiation stress by the lateral strain response method is to identify the crack damage stress. Utilizing the lateral strain response method to

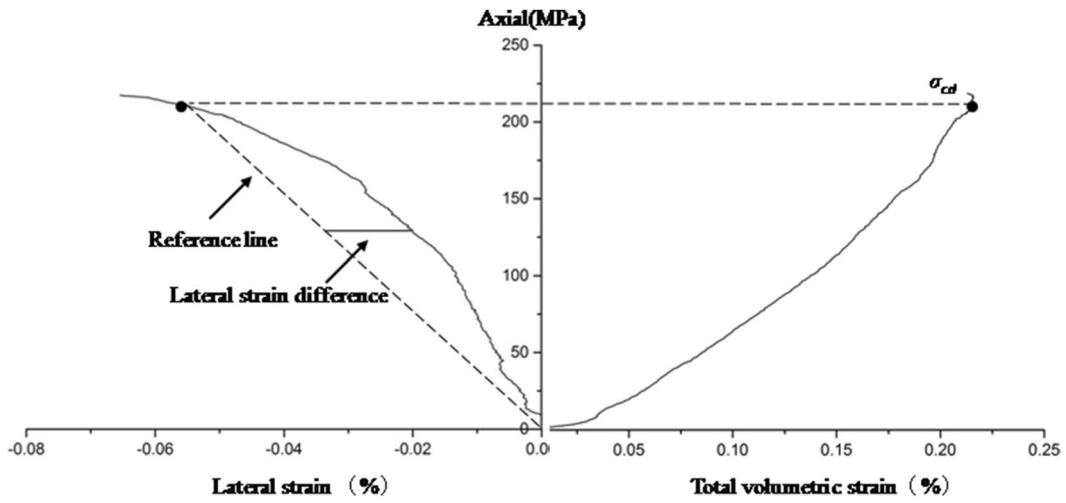

Fig. 5 Principle of the lateral strain response method

obtain the crack initiation stress, the determination of the maximum value of the lateral strain difference is unique in its use of data fitting to determine the extreme value, and human error is avoided. As seen from Fig. 6, the method to calculate the crack initiation stress (σ_{ci}) is relatively objective. The crack initiation stress (σ_{ci}) is 64% (siliceous siltstone) and 55% (limestone) of the peak stress. As seen from Fig. 6, the value obtained using the LSR is much larger than that using the CVS. When the specimen starts loading, the slope of the initial lateral strain curve of the specimen is larger than the slope of the reference line. The lateral strain difference peak point is the point where the slope of the tangent strain curve is the same as the slope of the reference line, so the elastic deformation section must be below the peak point of the lateral strain difference. This method does not explain the physical meaning, and the crack initiation stress is larger than the above CVS result.

3.3 Moving Point Regression Method (MPR)

Eberhardt et al. (1998) proposed a new method to obtain the crack closure stress (σ_{cc}) and the crack initiation stress (σ_{ci}). The volumetric stiffness (Fig. 7) is calculated from the volumetric strain divided by the axial stress. As the cracks close, the volumetric stiffness rapidly increases. The volumetric strain and volumetric stiffness curves during crack closure are non linear, followed by a linear region, and the slope represents the rate of change. This breakthrough of the slope represents a shift from crack closure to an approximately linear elastic behavior, and a further slope mutation represents the transition from a linear segment to the crack initiation and stable crack growth segment. It is well known that the reversal point of the volumetric strain curve represents the loading of the rock specimen into the unstable crack growth segment. This reversal point indicates the point at which the volumetric stiffness curves from positive to negative.

As we can see in Fig. 7a, from the beginning of loading to approximately 53 MPa, the specimen is in the crack closure segment, and the volumetric stiffness curve increases with irregular fluctuation. After this loading phase, the curve

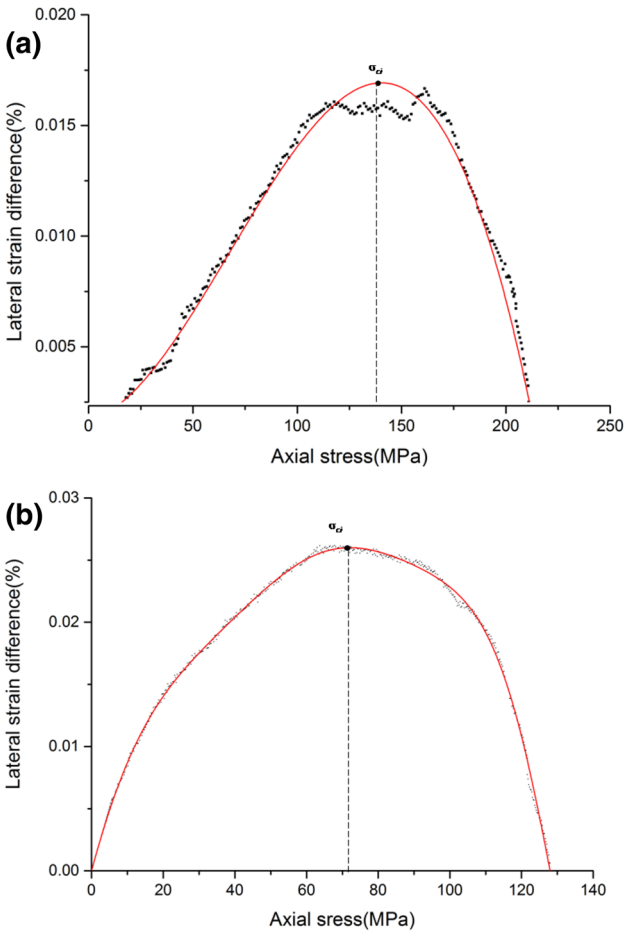

Fig. 6 Curves of lateral strain difference for **a** siliceous siltstone and **b** limestone

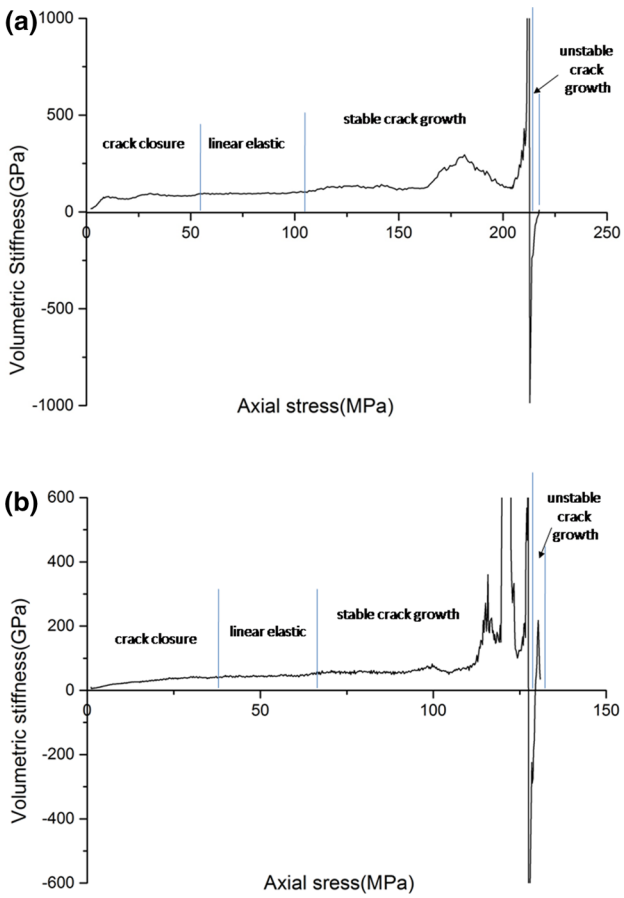

Fig. 7 Volumetric stiffness curves of **a** siliceous siltstone and **b** limestone obtained by the moving point regression technique

enters the linear segment. When the loading force reaches approximately 110 MPa, the curve begins to change irregularly. This point is the onset of stable crack growth. Until the point of volumetric stiffness changes from positive to negative (crack damage stress), the specimen loads into the unstable crack growth segment.

The final stress thresholds were 24% (σ_{cc}/σ_f) and 50% (σ_{ci}/σ_f) (siliceous siltstone), 30% (σ_{cc}/σ_f) and 50% (σ_{ci}/σ_f) (limestone). Compared with the crack volumetric strain method, the method of the MPR to obtain the stress threshold avoids the influence of the corresponding deformation analysis of rock physical and mechanical parameters, such as Poisson's ratio. The disadvantage of the MPR method is that it still needs the key inflection point in the artificial analysis curve. The MPR method has not yet removed the influence of subjectivity.

3.4 AE Method

Acoustic emission parameters are an effective means to obtain the segment of rock in a rock compression test. The closure, generation and expansion of microcracks are accompanied by the occurrence of many acoustic emission activities. The ringdown counts are the number of times the signal exceeds the preset threshold datum. The purpose of setting a threshold datum is to distinguish fracture-related acoustic events from background noise, but this threshold must be below enough to detect the beginning of the micro fracturing process. The ringdown count is a valid parameter that can represent the segment of rock compression.

Figure 8 shows the evolution of acoustic emission ringdown counts during the rock compression test. There will also be some acoustic emission in the initial stage of specimen loading, which is caused by the closing of the preexisting cracks in the specimens. Barely ringing counts occur until the specimen is loaded to 110 MPa. However, once the specimen reaches 110 MPa, the ringdown counts begin to occur and continue to increase steadily. This method has good consistency with σ_{ci} calculated by both the crack volumetric strain method and moving point regression method. Starting from 200 MPa, the ringdown counts began to substantially increase. Many AE ringdown counts reflected the unstable growth of the crack, which is the onset of unstable crack growth (σ_{cd}). This result demonstrates that acoustic emission can be used as an effective means to confirm these obtained stress thresholds.

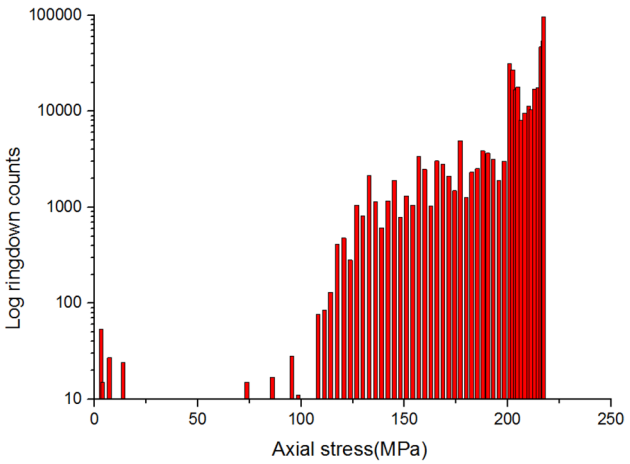

Fig. 8 Log acoustic emission response for a siliceous siltstone

4 Conclusion

These stress thresholds are important parameters for analyzing the deformation and failure of brittle rocks. If the stress level is lower than crack initiation stress (σ_{ci}), no damage occurred in the rock. If the stress level is higher than crack initiation stress (σ_{ci}) but lower than crack damage stress (σ_{cd}), cracks randomly initiated but they will cease at a certain length without coalescence. It is a stable cracking stage. If the stress level is higher than the crack damage stress (σ_{cd}) but lower than peak strength (σ_f), cracks will propagate continuously and coalescence to reach macroscopic failure. Based on the measured in situ stress and stress thresholds, we can predict the cracking condition and design support/grouting measures before excavation. Hence, it is important to determine the stress thresholds precisely.

In the present study, using strain gauge analysis and acoustic emission monitoring, a variety of methods is used to obtain the stress thresholds. The following observations were made with respect to uniaxial testing performed on specimens of siliceous siltstone and limestone:

1. When the stress thresholds are obtained by the crack volumetric strain method, the stress thresholds of these specimens are 47% (σ_{ci}/σ_f), 98% (σ_{cd}/σ_f) of peak stress (siliceous siltstone), and 50% (σ_{ci}/σ_f), 98% (σ_{cd}/σ_f) of peak stress (limestone).The crack volumetric strain method is a relatively objective method to obtain these stress thresholds, but its accuracy is easily affected by Poisson's ratio.
2. When utilizing the moving point regression technique to determine the stress thresholds, the measured cracking stress are approximately 24% (σ_{cc}/σ_f) and 50% (σ_{ci}/σ_f) (siliceous siltstone), 30% (σ_{cc}/σ_f) and 50% (σ_{ci}/σ_f) (limestone). There still are certain subjective factors, but this method is independent of Poisson's ratio. Thus, the stress threshold of the specimens can be more accurately obtained.
3. The lateral strain response method for crack initiation stress (σ_{ci}) can remove errors caused by human subjec-

tive factors. The crack initiation stress (σ_{ci}) is 64% (siliceous siltstone) and 55% (limestone) of the peak stress, which is larger than the crack volumetric strain method and the moving point regression technique. The physical meaning of this method is not yet clear, and its practicality requires further study.

4. Acoustic emission activity is monitored throughout the uniaxial compression test and can reflect the variation of the crack inside the rock to some extent. Therefore, the use of this activity is recommended as a supplementary strain measurement method to obtain the stress thresholds in the compression test.

It should be noted that these conclusions were drawn from only siliceous siltstone and limestone. In the future, more rock types should be tested and compared to see if they obey the same rule.

Acknowledgements The support provided by the National Natural Science Foundation of China (Grant nos. 51978541, 41941018, 51839009) is gratefully acknowledged. Many thanks are given to Mr. Chongyang Liu for assisting with the uniaxial compression tests.

Compliance with Ethical Standards

Conflict of interest The authors declare that they have no conflict of interest

References

Brace WF, Paulding BW, Scholz CH (1966) Dilatancy in the fracture of crystalline rocks. J Geophys Res 71:3939–3953

Cheng H, Zhou X, Zhu J, Qian Q (2016) The effects of crack openings on crack initiation, propagation and coalescence behavior in rock-like materials under uniaxial compression. Rock Mech Rock Eng 49:3481–3494

Dai F, Wei MD, Xu NW, Zhao T, Xu Y (2015) Numerical investigation of the progressive fracture mechanisms of four ISRM-suggested specimens for determining the mode I fracture toughness of rocks. Comput Geotech 69:424–441

Eberhardt E, Stead D, Stimpson B, Read RS (1998) Identifying crack initiation and propagation thresholds in brittle rock. Can Geotech J 35:222–233

Eberhardt E, Stead D, Stimpson B (1999) Quantifying progressive pre-peak brittle fracture damage in rock during uniaxial compression. Int J Rock Mech Min Sci 36:361–380

Hallbauer DK, Wagner H, Cook NGW (1973) Some observations concerning the microscopic and mechanical behaviour of quartzite specimens in stiff, triaxial compression tests. J Rock Mech Min Sci Geomech Abstr 10:713–726

Hoek E, Bieniawski ZT (1965) Brittle fracture propagation in rock under compression. Intl J Fract Mech 1:137–155

Lajtai EZ (1974) Brittle fracture in compression. Int J Fract 10:525–536

Liu QS, Wei L, Lei GF, Liu Q, Peng XX (2018) Experimental study on damage strength of crack initiation and evaluation of brittle parameters of sandstone. Chin J Geotech Eng 40:1782–1789

Martin CD, Chandler NA (1994) The progressive fracture of Lac du Bonnet granite. J Rock Mech Min Sci Geomech Abstr 31:643–659

Nicksiar M, Martin CD (2012) Evaluation of methods for determining crack initiation in compression tests on low-porosity rocks. Rock Mech Rock Eng 45:607–617

Scholz CH (1968) Experimental study of the fracturing process in brittle rock. J Geophys Res 73:1447–1454

Tapponnier P, Brace WF (1976) Development of stress-induced microcracks in Westerly granite. Int J Rock Mech Min Sci Geomech Abstr 13:103–112

Wawersik WR, Brace WF (1971) Post-failure behavior of a granite and diabase. Rock Mech Rock Eng 3:61–85

Yang SQ (2016) Experimental study on deformation, peak strength and crack damage behavior of hollow sandstone under conventional triaxial compression. Eng Geol 213:11–24

Yang SQ, Hu B (2019) Creep and long-term permeability of a red sandstone subjected to cyclic loading after thermal treatments. Rock Mech Rock Eng 52:297

Yang SQ, Huang YH, Ranjith PG (2018) Failure mechanical and acoustic behavior of brine saturated-sandstone containing two pre-existing flaws under different confining pressures. Eng Fract Mech 193:108–121

Zhang XP, Wong LNY (2013) Crack initiation, propagation and coalescence in rock-like material containing two flaws: a numerical study based on bonded-particle model approach. Rock Mech Rock Eng 46:1001–1021

Zhang Q, Zhang XP (2017) A numerical study on cracking processes in limestone by the b-value analysis of acoustic emissions. Comput Geotech 92:1–10

Zhang XP, Wong LNY, Wang SJ, Han GY (2011) Engineering properties of quartz mica schist. Eng Geol 121:135–149

Zhang XP, Zhang Q, Wu SC (2017) Acoustic emission characteristics of the rock-like material containing a single flaw under different compressive loading rates. Comput Geotech 83:83–97

Zhao X, Wang J, Ma LK, Su R, Cai M, Wang G (2012) Acoustic emission behaviors of the Beishan granite under uniaxial and triaxial compression conditions. In: The ISRM commission on design methodology. rock characterisation, modelling and engineering design methods-proceedings of the 3rd ISRM sinorock symposium. https://doi.org/10.1201/b14917-12

Zhou XP, Cheng H, Feng YF (2014) An experimental study of crack coalescence behaviour in rock-like materials containing multiple flaws under uniaxial compression. Rock Mech Rock Eng 47:1961–1986

Zhou XP, Bi J, Qian QH (2015) Numerical simulation of crack growth and coalescence in rock-like materials containing multiple pre-existing flaws. Rock Mech Rock Eng 48:1097–1114